JOURNAL OF GEOPHYSICAL RESEARCH, VOL. 102, NO. D19, PAGES 23,277–23,287, OCTOBER 20, 1997

Factors controlling threshold friction velocity in semiarid and arid areas of the United States

Beatrice Marticorena and Gilles Bergametti

Laboratoire Interuniversitaire des Systèmes Atmosphériques, University of Paris 12, Créteil, France

Dale Gillette

Air Resources Laboratory, NOAA, Research Triangle Park, North Carolina

Jayne Belnap

National Biological Service, Moab, Utah

Abstract. A physical model was developed to explain threshold friction velocities u_{*_t} for particles of the size 60-120 μm lying on a rough surface in loose soils for semiarid and arid parts of the United States. The model corrected for the effect of momentum absorption by the nonerodible roughness. For loose or disturbed soils the most important parameter that controls u_{*_t} is the aerodynamic roughness height z_0. For physical crusts damaged by wind the size of erodible crust pieces is important along with the roughness. The presence of cyanobacterial-lichen soil crusts roughens the surface, and the biological fibrous growth aggregates soil particles. Only undisturbed sandy soils and disturbed soils of all types would be expected to be erodible in normal wind storms. Therefore disturbance of soils by both cattle and humans is very important in predicting wind erosion as confirmed by our measurements.

1. Introduction

In arid and semiarid areas, soil erosion by wind is an important process that affects both the surface features and the biological potential of soils. The fluxes of wind-transported soil nutrients result in enrichment or impoverishment of the biological potential. Vigorous wind erosion leads to topographic changes, altering the conditions for plants and animals, examples of such changes in topography are the formation of sand dunes or the removal of whole soil horizons. Wind erosion can result in sandblasting of plants which can affect ecosystems.

In addition, emitted dust has a significant residence time in the atmosphere and acts to modify the radiative properties of the atmosphere, mainly by backscattering the incoming solar radiation [*Andreae*, 1996]. Different land uses in arid and semi arid areas (for example, overgrazing and dirt roads) and the possible climatic modifications can drastically change the dust emissions to the atmosphere [*Tegen et al.*, 1996].

Assessing the impact of dust emissions requires a framework for organizing interactions and identifying the importance of various mechanisms. This is a complex task because wind erosion involves nonlinear and threshold processes. A very important parameter in wind erosion is the threshold wind friction velocity u_{*_t} because it controls both the frequency and intensity of erosion events. Our goal here is to identify the main factors controlling variability of threshold wind friction velocities for arid and semiarid areas.

Our strategy was to measure threshold friction velocities, the aerodynamic roughness heights, and the size distribution of the soil particles for exposed soils of an area undergoing desertification. Our primary study site was the Jornada del Muerto experimental range (JdMER) located 37 km north of Las Cruces, New Mexico, U.S.A. JdMER is part of the area considered in the desertification studies of the Jornada del Muerto Long Term Ecological Research Project [*Havstad and Schlesinger*, 1996]. To complement this data set, we also used measurements taken in several other semiarid and arid areas of the United States (California, Nevada, Texas, and Colorado) by *Gillette et al.* [1982].

We first examined consistent patterns between threshold friction velocity and other observed parameters. Second, we tested whether the model proposed by *Marticorena and Bergametti* [1995] could explain the variability of observed threshold friction velocity. This model is mainly based on a parameterization of the threshold wind friction velocity as a function of the following soil surface features: the size distribution of the in situ erodible aggregates and the aerodynamic roughness length of the surface. It was shown that this parameterization satisfactorily simulates the erosion threshold wind friction velocities measured in a wind tunnel on natural bare soils [*Gillette, et al.*, 1980; *Nickling and Gillies*, 1989]. The tested soils ranged from smooth erodible surfaces to rough surfaces well protected from erosion.

Finally, we examined whether additional information such as the presence of cyanobacterial-lichen soil crusts (CLC) and other field parameters could help explain the observations. CLCs are found widely in most arid and semiarid landscapes throughout the world [*West*, 1990; *Belnap and Gillette*, 1997]. Studies suggest that these biotic crusts reduce damage by wind erosion for soil surfaces [e.g., *Williams et al.*, 1995].

2. Experiment

Because our purpose was to find the most important mechanisms controlling u_{*_t}, we measured the widest variety of soil types and surface features available at the JdMER study site.

Paper number 97JD01303.
0148-0227/97/97JD-01303$09.00

We used a generalized soil map of the range and measured several examples of each surface type that had wind erosion potential. The experimental method for measuring threshold friction velocity and aerodynamic roughness height was the same at all sites.

2.1. Site Description

All measurements of threshold velocity and aerodynamic roughness height were carried out at the Jornada del Muerto experimental range (JdMER). The experimental range includes mountains, dunes, playas, grassy areas, and mesquite-dominated vegetation and is representative of about 10.5×10^6 ha of the Chihuahuan Desert. The Chihuahuan Desert is located in southeastern Arizona, southern New Mexico, western Texas, and northern Mexico. The area of the range is 78,266 ha. Elevations range from 1260 to 2833 m. Surface materials include gravels washed from surrounding mountains at higher elevations, sandy soils dominant in intermediate elevations, and silts and clays in the lowest areas. The surface materials have little humus or organic matter. Alkalinity is high in all soil types. Although the area is classified as semidesert grassland, the actual vegetation cover is quite variable. Some areas have nearly pure stands of grass, other areas have savanna-like vegetation of grass interspersed with shrubs or trees, and yet other areas have nearly pure stands of shrubs.

A range scientist from the JdMER located typical examples of each of the soil classes chosen. These included sand, clay, silt, and gravel. Soils were singled out for special attention if they had large vegetation-free areas. He introduced the designation "playas" to distinguish these vegetation-free silt soils from vegetated silt soils. We also noted the presence or absence of CLC or physical rain crusts (PRC). These PRCs formed by the drying of soil following atmospheric precipitation wetting.

To work with data as widely representative as possible for arid and semiarid areas of the United States, we added the data of *Gillette et al.* [1982] from sites in the Mojave Desert of California and from sites in Nevada, Texas, and Colorado. The same wind tunnel, data reduction techniques and the same soil classifications used at these sites were used for JdMER. The total number of data points used from the JdMER was 110, and the number of points from the *Gillette et al.* [1982] paper was 35.

2.2. Threshold Measurements

A portable wind tunnel described by *Gillette* [1978] was used with an open-floored test section so that a variable-speed turbulent boundary layer could be developed over a flat soil containing small-scale roughness elements. The wind tunnel used a two-dimensional 5:1 contraction section with a honeycomb flow straightener and an expanding rectangular diffuser attached to the working section in a configuration similar to that of *Wooding et al.* [1973]. The working section was 15.2 cm^2 in cross section and 2.4 m in length. The wind tunnel was laid on areas free of vegetation. For most locations in the Jornada experimental range this was between plants. For some locations chosen, there were large areas of flat, vegetation-free soil. Wind data were obtained 20 cm from the end of the working section at the midpoint of the tunnel width at eight different heights spaced approximately logarithmically apart from 2 mm above the surface to 10 cm. The pitot tube anemometer was calibrated against the National Center for Atmospheric Research (NCAR) reference wind tunnel and was corrected for air density change caused by elevation above sea level. Data for the wind profiles were fitted to the function for aerodynamically rough flow [see *Sutton*, 1953].

$$U = \frac{u_*}{k} \ln\frac{z}{z_0} \tag{1}$$

where k is von Karman's constant (set to 0.4), U is mean wind speed, z is height above the surface, u_* is friction velocity, and z_0 is aerodynamic roughness height.

The threshold wind speed for wind erosion was defined to be that speed at which we observed small but continuing movement of particles across the soil surface. After slowly increasing the wind to the threshold of particle motion we obtained two sets of wind speed profiles. The following threshold profiles were obtained for each site: (1) For crusted soils (either CLC or PRC) we measured the threshold for loose particles on the surface and for the destruction of the crust. The playa soils and clay soils had no loose particles on the surface; therefore only the breakup of the soil surface was measured. (2) At sites without crusts (CLC or PRC) the threshold for loose surface particles was measured. (3) At all sites, soils were disturbed using either a cow's hoof or one pass of a three-quarter-ton truck moving at a speed of about 8 km h^{-1}. This disturbance always created loose particles at the sites. Measurements were made of the loose-particle threshold immediately following the disturbance. For each site, two replicates of the threshold measurements were obtained.

2.3. Soil Size Distribution

At each site the top 1 cm of soil was collected. The dry weight of the sample varied from 25 to 50 g. We measured the size distribution of the soil in a disturbed state because we excavated and transported each soil sample. We used a dry sieving method described by *Chatenet et al.* [1996]. Samples were dried for 24 hours at 105°C, followed by cooling in a dessicator. Only the fraction smaller than 2 mm was investigated. The fraction greater than 2 mm was eliminated by slow hand sieving. The samples were then dry sieved into 12 size classes: 2000-1000, 1000-800, 800-500, 500-400, 400-315, 315-250, 250-200, 200-160, 160-100, 100-80, 80-63, and <63μm. We used a fitting procedure based on the adjustment of lognormal distributions to the observed mass collected on the sieves. This method minimized the differences between the simulated and observed populations for each size class [*Gomes et al.*, 1990; *Chatenet et al.*, 1996]. Each soil is thus represented by up to three populations, each being characterized by a weight, geometric mean, and geometric standard deviation.

A size distribution having n modes [Jaenicke, 1985] can be computed for each soil by

where

$$\frac{dM(D_p)}{dln(D_p)} = \sum_{j=1}^{n} \frac{M_j}{(2\Pi)^{0.5}\ln(\sigma_j)} \exp\left[\frac{(\ln D_p - \ln MMD_j)^2}{-2\ln^2\sigma_j}\right] \tag{2}$$

D_p diameter of a particle;
j reference for mode j;

M mass fraction;
M_j mass fraction represented by mode j;
MMD_j mass median diameter of mode j;
s_j standard deviation of mode j.

3. Threshold Wind Friction Velocity Model

From a physical point of view, particle motion is controlled by the forces acting on it. For a particle at rest these forces are weight, interparticle cohesion forces, and the wind drag and lift forces on the surface. The first two are size dependent; the last one depends on the transfer of the wind energy to the erodible surface. This is controlled by the presence of roughness elements on the surface. Together, the forces determine the minimum threshold friction velocity required to initiate particle motion (the friction velocity being defined as the square root of the ratio of surface stress to air density).

3.1. Threshold Friction Velocity Versus Soil Particle Size

A theoretical formulation of the threshold friction velocity can be established by considering the equilibrium of the forces acting on a spherical loose particle at rest on a bed of similar particles under an air flow stream. At the threshold of aeolian erosion the aerodynamic drag force overcomes the interparticle cohesion forces.

Experimental data from *Bagnold* [1941] and *Chepil* [1944] confirmed this size dependence but also revealed an increase of the threshold friction velocity values for the smallest particles This determines an optimum particle size (about 60 μm) for which the threshold friction velocity is minimum. On the basis of a large set of measured threshold friction velocities obtained in wind tunnels and involving various particle densities (0.21 - 11.35 g cm^{-3}) and diameters (12 - 1290 μm), *Iversen and White* [1982] proposed two numerical formulations to predict the saltation threshold friction velocity. The use of these equations has been simplified [*Marticorena and Bergametti*, 1995] by an expression for the Reynolds number $B = u_{*t} D_p/\nu$ where D_p is particle size and ν, is kinematic viscosity, in the following form:

$$B = aD_p^x + b \tag{3}$$

with a = 1331, b = 0.38, and x = 1.56 for $\rho_a = 0.00123$ g cm^{-3} and $\rho_p = 2.65$ g cm^{-3}. To be consistent with the dimensionless Reynolds number, a has a unit of cm^{-x}. By using this expression for the Reynolds number in the *Iversen and White* [1982] expressions one can compute u_{*t} as a function of the particle diameter for air and particle densities specified above.

For $0.03 < B \leq 10$

$$u_{*t}(D_p) = 0.129 \frac{\left[\frac{\rho_p g D_p}{\rho_a}\right]^{0.5}\left[1+\frac{0.006}{\rho_p g D_p^{2.5}}\right]^{0.5}}{[1.928(a D_p^x + b)^{0.092} - 1]^{0.5}} \tag{4}$$

For $B > 10$,

$$u_{*t}(D_p) = 0.12\left[\frac{\rho_p g D_p}{\rho_a}\right]^{0.5}\left[1+\frac{0.006}{\rho_p g D_p^{2.5}}\right]^{0.5} \cdot (1 - 0.0858\exp\{-0.0617[(a D_p^x + b) - 10]\})$$

where g is the acceleration of gravity, ρ_a is the density of air, and ρ_p is the density of the particle.

3.2. Parameterization of the Drag Partition

In natural situations the presence of nonerodible elements affects the erosion threshold in two ways: (1) roughness elements directly cover part of the surface and thus protect it from the aeolian erosion and (2) they also consume part of the wind momentum that will not be available to initiate particle motion. This leads to a decrease of the wind shear stress acting on the erodible surface and thus of the erosion efficiency. We use a physical scheme of the drag partition between the roughness elements and the erodible surface developed by *Marticorena and Bergametti* [1995], derived from an approach developed by *Arya* [1975].

This approach consists of assuming that an internal boundary layer (IBL) characterized by a logarithmic wind velocity profile develops between roughness elements that are not too closely spaced (roughness density < 0.05). For $z < \delta$

$$U(z) = \frac{u_{*s}}{k}\ln\left|\frac{z}{z_{0s}}\right| \tag{5}$$

where u_{*s} is the small-scale friction velocity referred to the local shear stress, z_{0s} is the local roughness length of the uncovered smooth surface, and δ is the height of the internal boundary layer (IBL). For the surface as a whole z_0 is the large-scale roughness length.

The roughness length of the soil z_{0s} without any roughness elements can be estimated as $z_{0s} = D_{med}/30$ [*Greeley and Iversen*, 1985]. For the size range of particles most easily mobilized (60-120 μm), this relation provides roughness lengths ranging from 2×10^{-4} to 4×10^{-4} cm. Such values are consistent with measurements made in wind tunnels for smooth, loose soils [*Gillette et al.*, 1982; *McKenna-Neuman and Nickling*, 1994; *Li and Martz*, 1994].

The height of the IBL δ can then be defined as the height where the two profiles intersect. Thus, when the flow comes to an equilibrium with the surface, the wind velocity at the height δ satisfies both (1) and (5)

$$U(\delta) = \frac{u_*}{k}\ln\left[\frac{\delta}{z_0}\right] = \frac{u_{*s}}{k}\ln\left[\frac{\delta}{z_{0s}}\right] \tag{6}$$

The efficient friction velocity ratio f_{eff} is defined as the ratio of local to total friction velocity and can be written

$$f_{eff} = \frac{u_{*s}}{u_*} = 1 - \left[\frac{\ln[\frac{z_0}{z_{0s}}]}{\ln[\frac{\delta}{z_{0s}}]}\right] \tag{7}$$

The development of this IBL is assumed to be similar to the development of the IBL occurring after a sudden change in roughness, as described by *Elliott* [1958]. It is reasonable to assume that the flow does not immediately adjust to the new surface. The adjustment takes place gradually, and the height of the IBL δ increases with the distance downwind of the point of discontinuity of roughness as expressed by

$$\frac{\delta}{z_{0s}} = \alpha\left[\frac{x}{z_{0s}}\right]^{p} \tag{8}$$

where x is the distance downstream of the point of discontinuity of roughness. *Elliott* [1958] indicates that p is a constant and is equal to 0.8 over a large range of roughness lengths and that α depends on the ratio z_0 / z_{0s}. Field experimental data obtained by *Bradley* [1968] confirm (8) as well as the value 0.8 for p. Wind tunnel measurements from *Prendergrass and Arya* [1984] confirm (8) and indicate a value of 0.35 for α. Since the log profile that exists for very low ratios of height to Monin-Obukhov length is consistent with the *Prendergrass and Arya* [1984] wind tunnel measurements, we have used their value for α. The applicability of (8) to the developing IBL between two obstacles of a rough surface has been further confirmed by *Alfaro and Gomes* [1995] on the basis of wind tunnel experiments. For various surface roughness conditions they confirm values of 0.8 and 0.35 for p and a for neutral conditions.

Since δ is dependent on the distance downstream of the roughness element, f_{eff} is not constant. The local shear stress increases until an equilibrium value is eventually reached. A rigorous computation should integrate this variation along the distance between the roughness elements. However, for the sake of simplicity we have tested the possibility of using a mean value for δ to estimate the efficient ratio over a large range of roughness lengths [*Marticorena and Bergametti*, 1995]. Various numerical simulations were performed for roughness elements varying from 2.2 to 20 cm height and spacing from a few to hundreds of centimeters, corresponding to roughness density from 0.001 to 0.2 cm. For each simulated situation the mean value of f_{eff} was rigorously computed and compared with the values obtained for $x = 10$ cm. These results showed that f_{eff} is not very sensitive to x but is mainly dependent on the values of the roughness lengths. This is explained by the fact that the equilibrium value of f_{eff} is reached very rapidly after the obstacle, leading to a mean f_{eff} close to this equilibrium value. Thus the drag partition parameterization is expressed by

$$f_{eff} = \frac{u_{*s}}{u_*} = 1 - \left\{ \frac{\ln\left[\frac{z_0}{z_{0s}}\right]}{\ln\left[0.35\left(\frac{10}{z_{0s}}\right)^{0.8}\right]} \right\} \tag{9}$$

where z_0 and z_{0s} have units of centimeters. The value of $x = 10$ cm follows from computational tests by *Marticorena et al.* [1997], where the value of f_{eff} was computed and compared to the values obtained with x varying from 1 to 100 cm. The results showed that f_{eff} is not very sensitive to x but is mainly dependent on the values of the roughness length. The best agreement for the data used by *Marticorena et al.* [1997] was found by using $x = 10$ cm for the range of roughness height and density.

This expression was tested by simulating *Marshall's* [1971] measurements of the total and local wind shear stress for roughness lengths varying from 0.0001 to 0.1 cm. Marshall's measurements were used to calculate f_{eff}. The comparison between the computed and the measured values shows that the proposed scheme gives a good representation of the wind drag partition between the surface and the erodible elements for $f_{eff} > 0.2$. This limit in f_{eff} approximately corresponds to the maximum roughness density of 0.05 indicated by *Arya* [1975] as a limit for the logarithmic wind profiles hypothesis to be applicable.

The quantity f_{eff} was derived by *Marticorena and Bergametti* [1995]. It is not strictly equal to a threshold ratio (for example, R_t of *Raupach et al.* [1993]), since it is not specifically derived for wind erosion. For that reason, f_{eff} was compared to [1971] measurements, shown in a plot by *Marticorena and Bergametti* [1995]. Marshall's measurements were of local and overall wind shear stress rather than of threshold ratio. Since *Raupach et al.* [1993] also used Marshall's measurement to validate his model for threshold ratio, we claim that our parameterization f_{eff} is as satifying as Raupach et al.'s R_t.

By combining the size-dependent equation established in section 3.1 and the efficient ratio defined above, we can obtain an expression for the threshold friction velocity in a rough situation

$$u_{*t}(D_p, z_0, z_{0s}) = \frac{u_{*ts}(D_p)}{f_{eff}(z_0, z_{0s})} \tag{10}$$

where $u_{*ts}(D_p)$ is given by (4).

4. Results

4.1. Threshold of Crust Not Reached

The highest speed of the wind tunnel did not move any particles or cause any observed surface damage for 13 tests, 5 of which were for PRC crusted soils and 8 of which were CLCs. Our wind tunnel has a maximum wind velocity at the working-section midpoint dependent on motor speed and friction, geometry of the turbine, and friction in the test section. This maximum speed averages about 40 m s^{-1} at 7.9 cm (the wind velocity profile being maximum at the height 7.9 cm). The u_* calculated by a logarithmic wind profile, observed z_0, and constant maximum speed at 7.9 cm agreed well with our u_* calculated from the observed wind profile at the maximum wind speed.

The crusted soils that were unaffected by the highest wind speeds developed by our wind tunnel were two playas (PRC) and sand or silt soil with CLC. Well-developed undisturbed CLC soils have been found to provide strong protection from wind erosion for soils over long time periods, of the order of tens of years and beyond [*Belnap and Gillette*, 1997].

Of the three PRC silt soils that were located at the JdMER, only one broke at u_{*_t} > 150 cm s^{-1}, well above the normal maximum observed friction velocities; the other two did not erode at all in our tunnel. These three soils had been previously studied [*Gillette*, 1988] for the durability of the physical crusts. The three PRC soils were sampled monthly for 14 months. Each sample of crust was measured for crustal thickness and modulus of rupture. Results were plotted versus the maximum amount of rain for a single storm during that month. For all three playa soils the crust thickness and modulus of rupture were quite constant for the 14 month period (about 1 cm thickness and slightly less than 100 kPa modulus of rupture), despite variability of rainfall that included a 5 month drought.

These tests showed, therefore, that for the climatic conditions that existed in the 14-month period (May 1985 to July 1986) the PRC playa soils are vulnerable to wind erosion only following the disturbance of cattle or man. Since CLC silt and sand soils have similar threshold friction velocities, we would claim a similar degree of protection because the biological structure remains during both wet and dry periods.

The range of mean wind speeds at 10 m required to equal the maximum wind stress of the wind tunnel is 55 - 83 m s^{-1} (198 - 299 km h^{-1}) for z_0 ranging from 10^{-5} to 10^{1} cm. These speeds are well above speeds normally experienced at 10 -m height for our sites. Therefore these soils cannot be considered to be wind erodible without external disturbances.

4.2. Threshold Friction Velocity Versus Aerodynamic Roughness Height

A plot of all results of the wind tunnel measurements of u_{*_t} versus z_0 for the experimental data is shown in Figure 1. The plot clearly shows that measurements are bounded on the low side of u_{*_t} by disturbed soils and undisturbed noncrusted soils. The boundary for the high side of u_{*_t} is given by the values of crusted soils (both CLC and PRC) whose threshold could not be reached. Therefore these measurements were not threshold measurements but simply the highest friction velocity that the wind tunnel equipment could reach, given its top engine speed and fully opened valves.

We can distinguish two kinds of behavior for the soils for which we reached a threshold. Loose soil (uncrusted, nonaggregated soil) and disturbed soil behaved consistently. Crusted soils, whether rain formed (PRC) or biologically formed (CLC), made up the other group. This group had more variability from soil to soil than did loose soil. Detailed discussion of these results is given in section 5.

4.3. Size Distribution of the Soil Samples

Table 1 gives the statistical parameters of the one to three populations characterizing each sampled soil. The size distributions of the various samples in each soil category are relatively similar. Except for the sample referred as Jornada Sandy (JSA) 10-12 the sandy soils are characterized by a fine population whose median diameter ranges from 144 to 189 μm and a coarser population whose median diameter varies from 247 to 402 μm. The silty soils exhibit a very fine population (77-80 μm) and a very coarse one (586-886 μm). A similar size distribution is observed for the site characterized by the presence of gravel on the surface. A medium population (340-430 μm) is observed for the playas, with two samples exhibiting a fine population (83-100 μm). The playa sample Jornada Playa (JPL) 3 also exhibits a very coarse population with a median diameter of 1000 μm.These results are consistent with the size distributions established for the same soil categories that originated from other arid or semiarid areas of the world [*Chatenet et al.*, 1996; *Khalaf*, 1989].

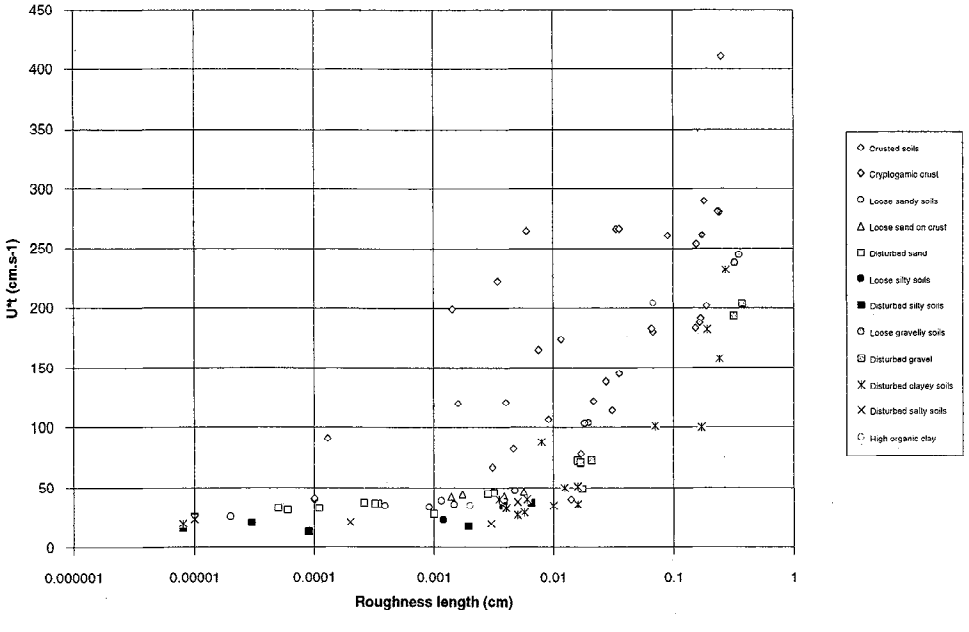

Figure 1. Values of u_{*_t} versus z_0 for tests at the Jornada del Muerto experimental range and for *Gillette et al.'s* [1982] data.

Table 1. Statistics of Multimodal Lognormal Size Distributions of Loose and Disturbed Soils for Which Threshold Friction Velocity Data Were Obtained

Soil Type	Reference	Population 1			Population 2			Population 3		
		%	Median, μm	GSD	%	Median, μm	GSD	%	Median, μm	GSD
Sand	JSA 1	10	189	1.20	90	402	2.11	-	-	-
	JSA 3	48	172	1.20	52	308	1.20	-	-	-
	JSA 5	62	187	2.64	38	247	1.45	-	-	-
		42	176	2.58	29	251	1.47	29	4000	1.20
	JSA 7-9	43	144	1.20	77	294	3.00	-	-	-
	JSA 10-12	10	80	1.20	90	199	2.65	-	-	-
Silt	JSI 1	20	77	1.75	80	886	3.00	-	-	-
	JSI 2	3	80	1.20	97	586	3.00	-	-	-
Playa	JPL1	100	340	2.73	-	-	-	-	-	-
	JPL 2	3	83	1.20	97	346	3.00	-	-	-
	JPL 3	3	100	1.20	48	430	3.00	49	1000	1.29
Clay	JCL1	20	60	1.36	18	188	1.20	62	486	2.16
Gravel	JGR	9	85	1.20	91	137	3.00	-	-	-
		32.7	87	2.02	20.9	612	3.00	46.4	4000	1.40

GSD is the geometric standard deviation; JSA is Jornada-Sandy; JSI is Jornada-Silty; JPL isJornada Playa; JCL is Jornada Clayey; and JGR is Jornada Gravel.

5. Discussion of Measurements of Threshold Friction Velocity Versus Aerodynamic Roughness Height

5.1. Disturbed and Uncrusted Soils and Loose Particles on Non-CLC Sand Crust

As illustrated in Figure 2, uncrusted soils, disturbed soils, and loose soil particles on sand PRC behave similarly. Threshold wind friction velocity increases exponentially with the roughness length, no matter what the soil type is. As a group, these threshold friction velocities were the lowest measured. For the same roughness length the threshold friction velocities reached for all loose and disturbed soils are of the same order of magnitude. Except for the gravelly soils and the high-organic clayey soils the disturbed soils exhibit a larger range of roughness length than do the loose soils. This may result from the presence of nonerodible pieces of crust mixed in with finer disturbed material. These disturbed soils are thus protected more efficiently from erosion than are the loose soils.

Gravelly material provides strong protection against wind erosion. Threshold friction velocities for gravelly soils were more than 100 cm s^{-1}. After hoof disturbance the minimum threshold friction velocity measured was 70 cm s^{-1}. This is seldom exceeded in nature. Vegetation is often found with gravelly sites, which would probably make wind erosion rare at those sites. The high-organic clayey soils acted similarly to the

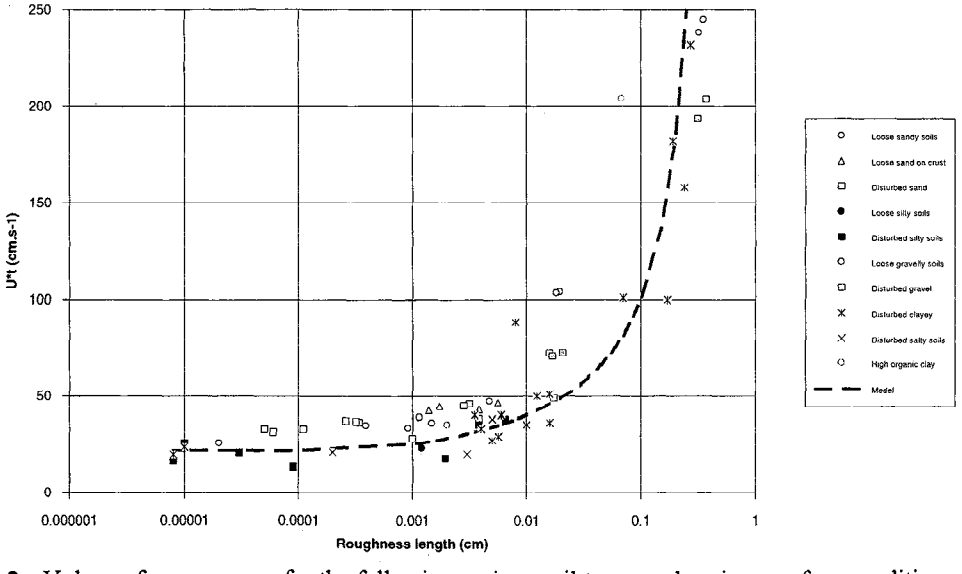

Figure 2. Values of u_{*_t} versus z_0 for the following various soil types and various surface conditions: loose (undisturbed soils), disturbed soils, and loose particles on the crust. The dashed line is for $u_{*_t} = 21.7$ cm s^{-1}, $z_{0s} = 4 \times 10^{-4}$ cm.

Table 2. Percentage of Particles Smaller Than 100 μm in the Soil Samples of Jornada del Muerto

Sample Reference	Percentage of Particles < 100μm
JSA 1	13.73
JSA 3	24.41
JSA 5	32.17
JSA 7-9	44.38
JSA 10-12	43.55
JGR	55.45
JSI 1	28.40
JSI 2	18.12
JPL 1	22.11
JPL 2	22.59
JPL 3	5.56
JCl 1	25.26

gravelly soils; that is, the clay aggregates broke into small blocks the size of gravel particles. Although the composition was clay, the size, hardness, and density were very similar to those of the gravelly soils.

To apply the threshold parameterization, we need information about the size of the soil particles whose movement was detected at threshold. *Iversen and White* [1982] observed that the minimum threshold friction velocity for eroding particles occurred between 60-120 μm in diameter. From the measured soil size distribution we computed the mass percentage of particles smaller than 100 μm in the soil samples of JdMER (Table 2). For most of the soils this ranges from 20 to 50%. These results show that particles in the optimal size range for erosion threshold are always observed in the soils. Thus we used a mean value of $u_{*_{ts}}$ of 21.7 cm s^{-1} corresponding to this size range (the "*s*" subscript standing for "smooth"). We estimated the smooth roughness z_{0s} as one thirtieth of the largest diameter of this optimal size range, which gives a value of 4×10^{-4} cm. Substituting $u_{*_{ts}} = 21.7$ and $z_{0s} = 4.1 \times 10^{-4}$ cm in (9) and (10), theoretical values of u_{*_t} can be computed for the range of measured "rough" z_0. This theoretical curve of u_{*_t} versus z_0 is plotted in figure 2.

Over the whole range of roughness lengths (1×10^{-5} to 0.37 cm), good agreement was obtained between the model and the experimental data, corresponding to threshold velocities ranging from 20 to 250 cm s^{-1}. Because of this agreement we deduced that the variations of the threshold wind friction velocity for the loose and undisturbed soils are controlled by the changes in the surface roughness. This affects the threshold velocity by partitioning the wind drag between the nonerodible elements and the erodible surface. Because of the presence in all these soils of particles in the optimal size range for wind erosion, the size of the erodible particles does not significantly influence the threshold velocity. This applies to all the loose and disturbed soils, despite their type. Consequently, "loose and disturbed soils" is our most erodible classification. The theoretical curve simulating the erosion threshold for this classification is effectively the lowest limit of erosion threshold at a given roughness length.

5.2. Crusts Damaged by Wind Erosion

This category of soil consists of both CLC and PRC crusted soils. What is called threshold for this category is a threshold of damage of the crust by the wind. The crusts that were damaged (either PRC or CLC) were cracked before testing; loose chunks or crust, flakes, or curls were torn away. For some of the JdMER sites this threshold corresponded to a slight damage of the crust; for the supplementary data, only extensive crust damage was recorded, and only PRC soils were tested. Our data set for crusted soils is thus divided in two categories: soils whose crust was damaged by wind and soils whose crust was only slightly damaged. The latter category includes only CLC soils, and the threshold corresponds to the movement of a few individual crust pieces. The first category corresponds to sandy, silty, or clayey soils. Normally, all sand PRC crusts could be destroyed by our wind tunnel, which is capable of u_{*_t} values of more than 100 cm s^{-1}. PRC crusts having silt or clay composition were more resistant to erosion than were sand PRC crusts. Clay PRCs are often curled or broken by natural desiccation, cracking into pieces that are vulnerable to high winds developed by the wind tunnel.

Figure 3 is a plot of u_{*_t} versus z_0 for both crusted soils. The experimental threshold exhibits only a weak relation with z_0. No clear trend is observed except for an increase of u_{*_t} with increasing z_0. For a given roughness length the range of measured threshold wind friction velocity is very large. However, almost all the points are located in the area delimited by the upper line, corresponding to the maximum capacity of the wind tunnel, and the lower line, corresponding to the theoretical model for loose soils. The behavior of the crusted soil cannot be explained by the previous theoretical curve that corresponds to a movement threshold controlled only by the roughness length. This suggests that the threshold of damaged crust is influenced by another factor.

To investigate a possible influence of the size of the mobilized pieces of crust, we decided to remove from the experimental value of threshold friction velocity the part of the variation caused by the change in the roughness length from one soil to the other. From our parameterization (10) the threshold wind friction velocity u_{*_t} results from the combination of a size-dependent threshold $u_{*_{ts}}(D_p)$ which accounts for the influence of the size-eroded elements and of the efficient fraction $f_{\text{eff}}(z_0, z_{0s})$ which represents the influence of the surface roughness. The size-dependent threshold friction velocity $u_{*_{ts}}(D_p)$ can thus be determined for each soil as the product of the measured u_{*_t} and the efficient fraction

$$u_{*_{ts}} = u_{*_t} \times f_{\text{eff}}.$$

We can thus estimate the $u_{*_{ts}}$ of the various soils by computing their respective efficient fractions f_{eff}. For this we computed the smooth roughness lengths from the size of the mobilized elements. For *Gillette et al.'s* [1982] data set the dimensions of the pieces of crust were given. The mean volumes of the pieces have thus been computed from the measured

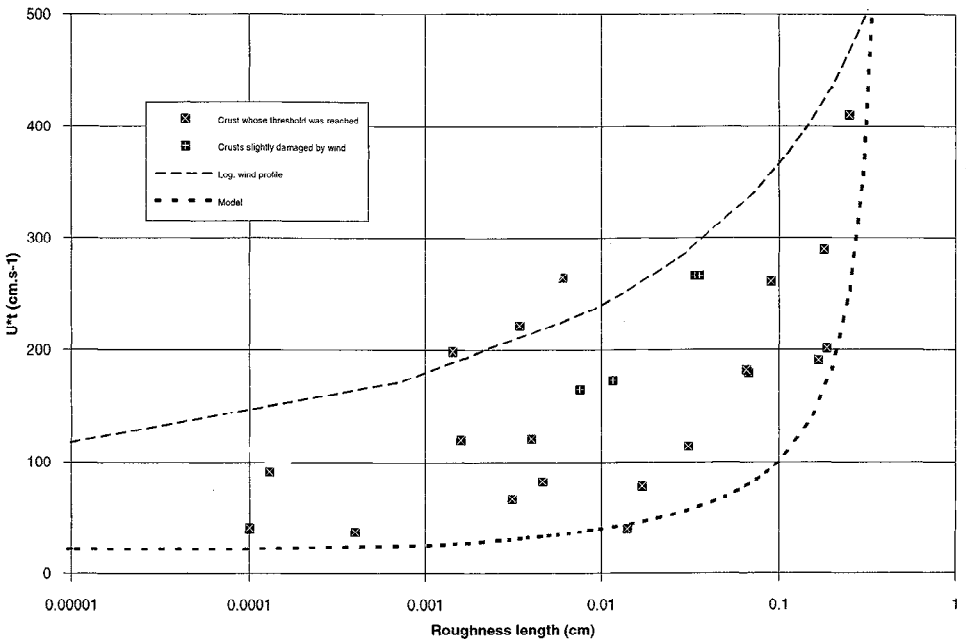

Figure 3. Values of u_{*_t} verdus z_0 for soils where the thresholds for crustal damage were reached. The long-dashed line shows the upper limit of u_{*_t} and the short-dashed line is the lowest limit for the exponential data simulated by the model (see Figure 3).

length, width, and thickness and "rescaled" to size dimension by taking the cube root of the computed volume. For the JdMER soils the sizes of the crust pieces were estimated from field notes and close-up photographs of the surfaces. We have used one thirtieth of the size of the pieces as a rough estimation of the smooth roughness length. When this computation provided a higher value than the measured roughness length, we retained the experimental result, assuming that no other elements than the mobilized pieces act to affect aerodynamic roughness height. From these computed roughness lengths and the measured ones we computed the efficient fraction.

Multiplying the measured threshold friction velocities by the computed efficient fraction provides an estimate of $u_{*_{ts}}$ for each PRC or CLC soil. In Figure 4 we plotted the estimated $u_{*_{ts}}$ versus

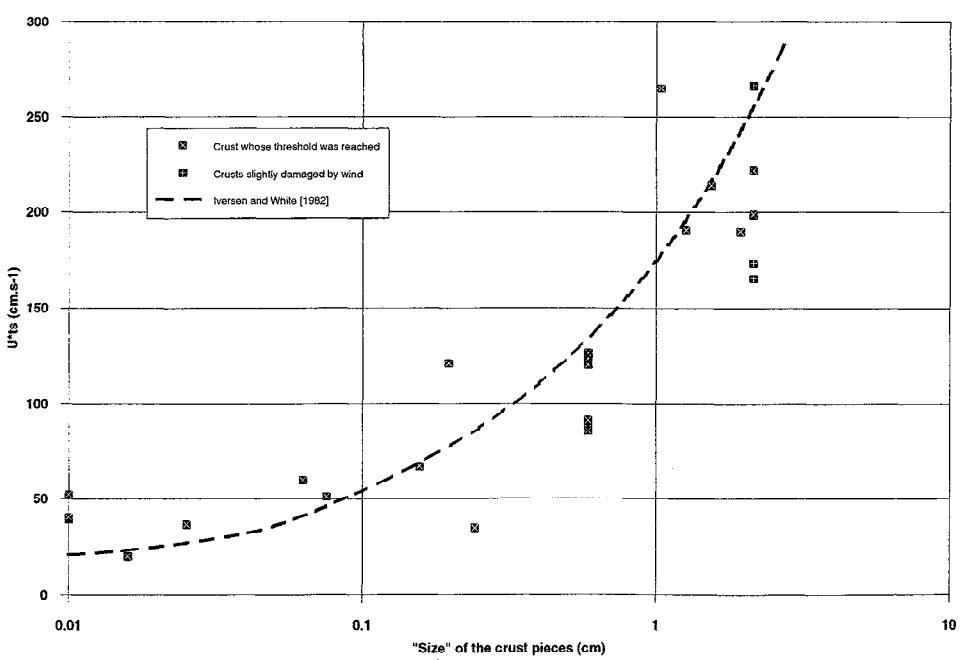

Figure 4. Observed $u_{*_{ts}}$ (u_{*_t} times f_{eff}, equivalent to the threshold friction velocity of the crust pieces) versus the equivalent size of a typical crust piece. Also shown is the theoretical curve of $u_{*_{ts}} = f(D_p)$, derived by *Iversen and White* [1982].

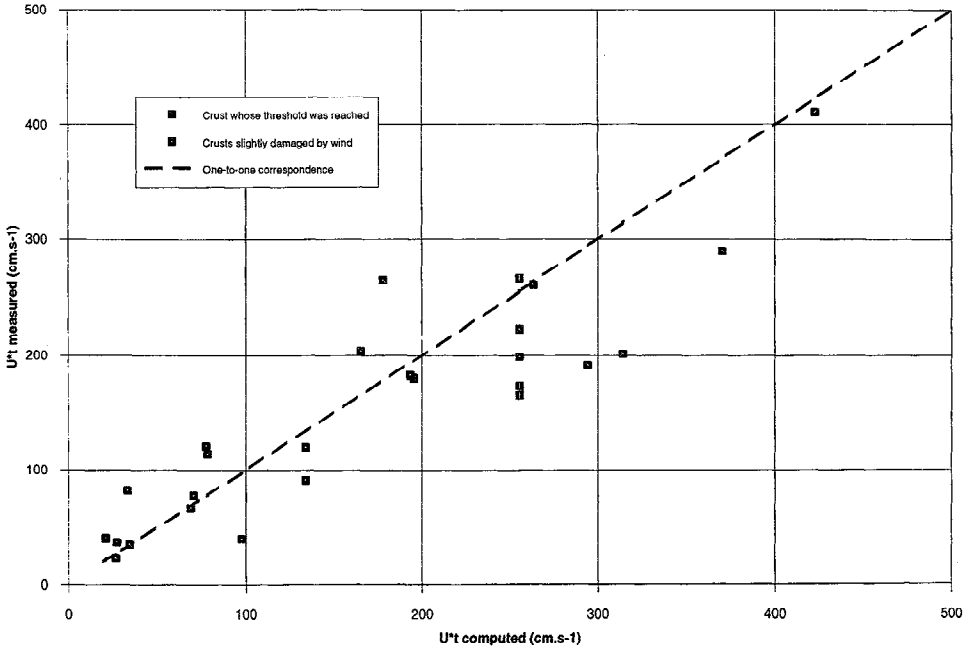

Figure 5. Computed u_{*_t} for crusts versus measured u_{*_t}. The dashed line is a one-to-one correspondence.

the size of the mobilized crust pieces. For comparison, the theoretical curve of $u_{*_{ts}} = f(D_p)$ derived from *Iversen and White* [1982] (our equation 4) was plotted on the same graph. Even if the data are sparse, the similarity with the theoretical curve is quite clear. The points showing the largest discrepancy with the theoretical curve correspond to the JdMER soils where the sizes of the pieces were not directly measured but estimated after the experiment from photographs. The discrepancies may also be due to the fact that we have used for the computation of $u_{*_{ts}}$ the same density as for individual grains, whereas it may be lower for large aggregates. This result suggests that the theoretical curves derived from *Iversen and White* [1982] can be used as an estimate of $u_{*_{ts}}$ for the PRC and CLC soils, providing the dimension of the crust pieces mobilized by the wind is known.

On the basis of the size of crust pieces we have computed theoretical values of $u_{*_{ts}}$ by using (4). By combining these theoretical $u_{*_{ts}}$ values and the efficient fraction computed as a function of z_0 we obtained an estimate of the total threshold friction velocity u_{*_t} for the crusted soils. In Figure 5 we have plotted the computed u_{*_t} values versus the measured threshold friction velocities. The agreement between the computation and the experimental data shows that the model provides a good estimate of the threshold of damage for the PRC and CLC soils.

For these soils the thresholds are governed by the combined effect of the surface roughness of the PRC and CLC and by the size of the crust pieces that can be mobilized. For the cases where the roughness is directly controlled only by the crust pieces, the size effect is dominant. For the other cases the relative weight of these two components depends on the considered range of roughness length and size of pieces. This behavior differs from the one observed for loose or disturbed soils because the size effect is quite negligible compared with the roughness effect.

The high threshold velocities measured for undisturbed PRC and CLC soils show the efficiency of soil crusting as a protection from wind erosion. Since crust threshold is strongly influenced by the size of the crust pieces, the size of cracking of natural crusts should be observed.

5.3. Soils With Cyanobacterial-Lichen Crust

Scanning electron microscope studies by *Belnap and Gardner* [1993] have shown the presence of extracellular, cyanobacterial sheath material that binds soil particles together. In threshold velocity tests of cyanobacterial-lichen crust (CLC) soils in southern Utah, *Belnap and Gillette* [1997] showed that these crusts were resistant to erosion, even during severe drought. The CLC soils, although brittle during drought, provided sufficient resistance to wind forces to prevent wind erosion. If the brittle matting of the CLC is fractured and dispersed, however, the protection of the CLC is destroyed. Because threshold measurements were made for samples with and without CLC and both under disturbed and undisturbed conditions, comparison of these data sets provides us the opportunity to document the effect of the CLC on these two soil types.

In Figure 6 the u_{*_t} versus z_0 values for loose particles on disturbed and undisturbed CLC crusts of both sand and silt composition are plotted along with values of disturbed silty PRC soils (playas), loose particles on PRC sand, and disturbed non-CLC sand. The experimental data show a clear increase of the threshold wind friction velocities for the CLC soils compared with all non-CLC soils; most of the CLC soils exhibit thresholds higher than 70 cm s^{-1} up to 270 cm s^{-1}. This increase is consistent with the measured roughness lengths; no CLC sand or silt has z_0 smaller than 0.08 cm, while no sand or silt without CLC has z_0 larger than this value. The increase of the thresholds of CLC soils can thus be interpreted as an effect of CLC to create surface roughness. Direct examination of the CLC soils shows that the organic matting acts to create a rougher surface than for sand or silt without CLC.

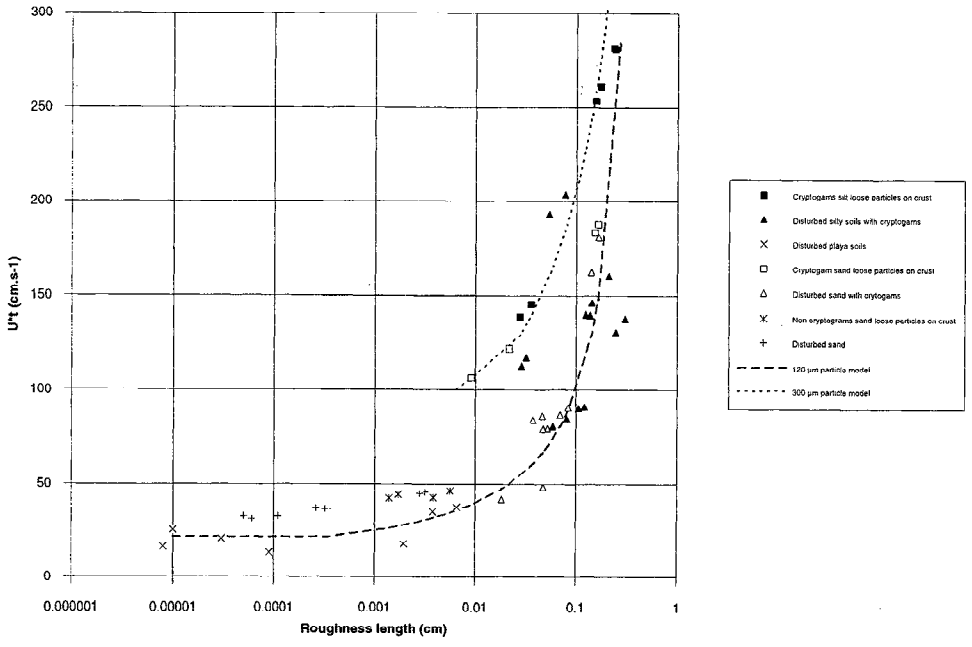

Figure 6. Observed u_{*_t} for loose soils and for loose particles on cyanobacterial-lichen soil crusts. The long-dashed line is the model for loose soil u_{*_t} (120 µm particles), and the short-dashed line is the model for 300 µm particles.

For the disturbed CLC soils the experimental data are simulated well by the theoretical model used to describe the behavior of the loose or disturbed soils without CLC. This result indicates that for the disturbed CLC sample the CLC acts only to increase the surface roughness.

The undisturbed CLC soils have larger thresholds than the disturbed CLC soils for the same roughness length. This suggests an additional effect to increase of surface roughness. The loose particles whose movements were detected on the undisturbed CLC crust are probably not loose soil particles but rather small pieces detached from the biotic crust. These aggregates, composed of individual soil particles bonded to each other with organic fibers, are coarser, possibly less dense and thus may require a larger u_{*_t} value at a given z_0. To reproduce these data with our parameterization, we decided to account for the size of the mobilized crust pieces in the computation of the $u_{*_{ts}}$. From examination of surface photographs we estimated these small crust pieces as having a size about 0.3 cm. This size provides a u_{*_t} value of 100 cm s^{-1} and a z_{0s} equal to 0.01 cm. From these values we have plotted a second theoretical curve that shows higher u_{*_t} for a given z_0 than our first curve also shown in Figure 2. Our second model curve accounts for both the size effect and the roughness effect. Regarding the number of data available for the undisturbed CLC soils, the agreement between the measured and computed thresholds can be considered as satisfactory.

The effects of CLC on soil wind erosion may be summarized by the following two points: (1) CLC soils are not damaged as much by the wind as are soils not having CLC. For sandy soils the effect of CLCs is especially clear; sandy soils are greatly protected from wind erosion by CLC. (2) When CLCs are disturbed, part of the protective effect is destroyed. The dried CLC is easily crushed and broken into fine powder by disturbance. Consequently, aggregates are partially destroyed and loose particles in the size range 60-120 µm are generated. However, in our tests some of the surface roughness survives the disturbance, so that protection by surface roughness is still present, although to a reduced degree.

6. Conclusions

The above analysis provides a hierarchy of mechanisms controlling the threshold friction velocities measured on various soils of semiarid and arid areas of the United States. First, for loose or disturbed soils the most important parameter that controls u_{*_t} is roughness of the surface that is conveniently parameterized by the aerodynamic roughness height z_0. The roughness acts to absorb part of the momentum of the wind. The soil size distribution has a limited effect because in our observations there is a sufficient quantity for all our soils of particles that correspond to the minimum threshold. Second, for the PRC or CLC crust that can be damaged by wind, the size of erodible units is important along with the roughness. In this case the thickness and area of detachable PRC or CLC crustal units define a size D_p where $u_{*_t}(D_p)$ changes rapidly for small changes in D_p. Third, the presence of cyanobacterial-lichen soil crusts increases the threshold in two ways: the crusting roughens the surface and the biological fibrous growth aggregates soil particles even after the crust is dry and even when the biological material is dead. Consequently, the CLC are good protectors of the soil against wind erosion when undisturbed. When disturbed, the CLC loses most of its protective qualities, since disturbance flattens the roughness and breaks the brittle aggregates.

On the basis of our measurements, only undisturbed sandy soils and disturbed soils of all types would be expected to be erodible. Because vegetation also is a protector of the soil from wind erosion, vegetation patterns are very important for the erosion of all soil types. Finally, our measurements point to the patterns of disturbance by both cattle and by humans as being of primary importance in making predictions of wind erosion.

Acknowledgments. The authors gratefully acknowledge Bob Gibbens for sharing his great knowledge of the Jornada del Muerto and for his help in selecting experiment sites. Kris Havsted, director of the Jornada del Muerto experimental range, was extremely helpful in all steps of this project. John Dunaway and Linda Sperry provided field support and helpful discussions. Dale Gillette was partially supported by the Centre National de la Recherche Scientifique during June-September 1996; Jayne Belnap was supported by the Environmental Division, U. S. Army Corps of Engineers. This research was carried out as part of the Long Term Ecological Research (LTER) program at the Jornada del Muerto site. The Jornada del Muerto LTER project is administered by Duke University and is supported by the National Science Foundation grant DEB 94-11971.

References

Alfaro, S. C., and L. Gomes, Improving the large-scale modeling of the saltation flux of soil particles in presence of nonerodible elements, *J. Geophys. Res., 100*, 16,357-16,366, 1995.

Andreae, M. O., Raising dust in the greenhouse, *Nature, 380*, 389-390, 1996.

Arya, S. P. S., A drag partition theory for determining the large-scale roughness parameter and wind stress on Arctic pack ice, *J. Geophys. Res., 80*, 3447-3454, 1975.

Bagnold, R. A., *The Physics of Blown Sand and Desert Dunes*, 265 pp., Methuen, New York 1941.

Belnap, J., and J. Gardner, Soil microstructure of the Colorado Plateau: The role of the cyanobacterium *Microcoleus vaginatus*, *Great Basin Nat., 53*, 40-47, 1993.

Belnap, J., and D. Gillette, Soil surface disturbance impacts on potential wind erodibility of sandy desert soils in SE Utah, USA, *Land Degradation*, in press 1997.

Bradley, E. F., A micrometeorological study of velocity profiles and surface drag in the region modified by a sudden change in surface roughness, *Q. J. R. Meteorol. Soc., 94*, 361-379, 1968.

Chatenet, B., B. Marticorena, L. Gomes, and G. Bergametti, Assessing the size distribution of desert soils erodible by wind, *Sedimentology, 43*, 901-911, 1996.

Chepil, W. S., Utilization of crop residues for wind erosion control, *Sci. Agric., 24*, 307-319, 1944.

Elliot, W. P., The growth of the atmospheric internal boundary layer (abstract), *EOS Trans. AGU, 39*, 1048-1054, 1958.

Gillette, D., Tests with a portable wind tunnel for determining wind erosion threshold velocities, *Atmos. Environ., 12*, 2309-2313, 1978.

Gillette, D. A., Threshold friction velocities for dust production for agricultural soils, *J. Geophys. Res., 93*, 12,645-12,662, 1988.

Gillette, D., J. Adams, A. Endo, D. Smith, and R. Kihl, Threshold velocities for input of soil particles into the air by desert soils. *J. Geophys. Res., 85*, 5621, 5630, 1980.

Gillette, D., J. Adams, D. Muhs, and R. Kihl, Threshold friction velocities and rupture moduli for crusted desert soil for the input of soil particles into the air, *J. Geophys. Res., 87*, 9003-9015, 1982.

Gomes, L., G. Bergametti, G. Coudé-Gaussen, and P. Rognon, Submicron desert dust: A sandblasting process, *J. Geophys. Res., 95*, 13,927-13,935, 1990.

Greeley, R., and J. D. Iversen, *Wind as a Geological Process on Earth, Mars, Venus and Titan*, 333 pp., Cambridge Univ. Press, New York 1985.

Havstad, K., and W. Schlesinger, Reflections on a century of rangeland research in the Jornada Basin of New Mexico, In *Proceedings of the Symposium on Shrubland Ecosystem Dynamics in a Changing Climate*, edited by J. R. Barrow *et al.*, U.S. For. Ser., Ogden, Utah, 1996.

Iversen, J. D., and B. R. White, Saltation threshold on Earth, Mars and Venus, *Sedimentology, 29*, 111-119, 1982.

Jaenicke, R., Aerosol physics and chemistry, in *Meteorology, Landolt-Borstein New Ser.*, vol. 4, edited by G. Fischer, pp. 391-457, Springer-Verlag, New York, 1985.

Khalaf, F., Textural characteristics and genesis of the aeolian sediments in the Kuwaiti desert, *Sedimentology, 36*, 253-271, 1989.

Li, L. and L. W. Martz, System of numeric models for sand particle transport by wind, *J. Geophys. Res., 99*, 12,999-13,012, 1994.

Marshall, J. K., Drag measurements in roughness arrays of varying density and distribution, *Agric. Meteorol., 8*, 269-292, 1971.

Marticorena, B., and G. Bergametti, Modeling the atmospheric dust cycle, 1, Design of a soil-derived dust emission scheme, *J. Geophys. Res., 100*, 16,415-16,430, 1995.

Marticorena, B., G. Bergametti, B. Aumont, Y. Callot, C. N'Doume, and M. Legrand, Modeling the atmospheric dust cycle: 2. Simulation of Saharan dust sources, *J. Geophys. Res., 102*, 4,387-4,404, 1996.

McKenna-Neuman, C., and W.G. Nickling, Momentum extraction with saltation: Implications for experimental evaluation of wind profile parameters, *Boundary Layer Meteorol., 68*, 35-50, 1994.

Nickling, W. G., and J. A. Gillies, Emission of fine-grained particulates from desert soils, in *Paleoclimatology and Paleometeorology: Modern and Past Patterns of Global Atmospheric Transport*, edited by M. Leinen and M. Sarthein, pp. 133-165, Kluwer Acad., Norwell, Mass., 1989.

Prendergrass, W., and S. P. S. Arya, Dispersion in neutral boundary layer over a step change in surface roughness, I, Mean flow and turbulence structure, *Atmos. Environ., 18*, 1267-1279, 1984.

Raupach, M., D. Gillette, and J. Leys, The effect of roughness elements on wind erosion threshold, *J. Geophys. Res.*, 98, 3023-3029, 1993.

Sutton, O. G., *Micrometeorology*, 333 pp. McGraw-Hill, New York 1953.

Tegen, I., A. A. Lacis, and I. Fung, The influence on climate forcing of mineral aerosols from disturbed soils, *Nature, 380*, 380-384, 1996.

West, N. E, Structure and function of soil microphytic crusts in wildland ecosystems of arid and semi-arid regions: *Adv. Ecol. Res. 20*, 179-223, 1990.

Williams, J., J. Dobrowolski, N. West, and D. Gillette, Microphytic crust influence on wind erosion, *Trans. ASAE, 38*, 131-137, 1995.

Wooding, R., E. Bradley, and J. Marshall A low-speed wind tunnel for model studies in micrometeorology, *Boundary Layer Meteorol., 5*, 285-308, 1973.

J. Belnap, National Park Service, 2282 S. West Resource Blvd, Moab, UT 84532.

G. Bergametti and B. Marticorena, Laboratoire Interuniversitaire des Systèmes Atmosphériques, URA CNRS 1404, Université Paris VII et XII, Centre Multidisciplinaire de Créteil, 61 avenue du Général de Gaulle 94010 Crétceil cedex, France. (e-mail: bergametti@univ-paris12.fr; marticorena@univ-paris12.fr).

D. Gillette, Atmospheric Sciences Modeling Division, Air Resources Laboratory, NOAA, Research Triangle Park, NC 27711.

(Received January 21, 1997; revised April 25, 1997;
accepted April 30, 1997.)